

Sedimentation of active particles

Jérémy Vachier* and Marco G. Mazza†

Max Planck Institute for Dynamics and Self-Organization, Am Fassberg 17, 37077 Göttingen, Germany

(Dated: May 18, 2022)

Active particles convert energy from chemical, biochemical, or other processes into motion. Their collective motion has attracted enormous interest on account of the technological applications of artificial and biological particles. By combining theoretical arguments, and molecular dynamics simulations we explore the collective behavior of active particles under a gravity field in three dimensions. Dilute systems exhibit sedimentation, which we study with two approaches. Firstly, we solve analytically the associated Fokker–Planck equation, which gives us access to the full temporal evolution of the system. Secondly, we carry out molecular dynamics simulations for many particles under the effect of gravity. The density profile and its dependence on the effective diffusivity agree well with experiments.

I. INTRODUCTION

The study of active particles, and especially their collective motion, has received much attention due to a renewed interest in the physical principles underlying the motion of, *e.g.*, plankton or bacteria, and also in light of technological application involving both biological and artificial controllable active systems [1–3]. Active particles exhibit a fascinating multitude of interesting behaviors from the single particle to collective states [4–6], due to the nonequilibrium nature of the active particles. Even in dilute suspensions, where interactions among active particles can largely be neglected, and the dynamics are dominated by the balance of active motion and gravity, interesting results are found [7–10]. Palacci *et al.* [11] found in experiments with active colloids that the density profile decays exponentially with distance from the bottom solid surface where they sediment, and that the active motion changes the effective diffusivity and increases the sedimentation length. More recently, Ginot *et al.* [12] characterized the equation of state of sedimenting active colloids as a function of the activity.

Theoretical studies of active particles, based on the framework of active Brownian particles [13] and stochastic processes, have mostly focused on two-dimensional systems [14–17]. A complete description in three-dimensions in terms of the Fokker–Planck equation is challenging [18, 19] and some recent progress in the theory of one active particle [8, 20, 21], highlights the fact that many questions are still open especially in three-dimensions.

In this work we aim to analytically characterize the sedimentation of active particles in three dimensions for one particle, and, by means of molecular dynamics simulations for many weakly-interacting particles. First, we analytically describe the sedimentation of one active particle under gravity, with two first-order stochastic differential equations and the associated Fokker–Planck equation to obtain the particles’ density profile in the direction of gravity. The density profile is obtained from the probability density function $\mathcal{P}(\mathbf{r}, \mathbf{e}, t | \mathbf{r}_0, \mathbf{e}_0, t_0)$ of finding an active particle at the position \mathbf{r} , with an orientation \mathbf{e} at time t , given the initial state $(\mathbf{r}_0, \mathbf{e}_0, t_0)$. Due to the complexity of the problem, finding the general expression of $\mathcal{P}(\mathbf{r}, \mathbf{e}, t | \mathbf{r}_0, \mathbf{e}_0, t_0)$ in three dimensions is challenging. However, the method presented here allow us to keep the coupling between the orientation and the position obtained in three-dimension, which we then specialize in one-direction. Secondly, we perform molecular dynamics simulations to describe the sedimentation of many particles, where fluid-mediated hydrodynamic interactions are approximated via a short-range potential with up-down symmetry.

II. METHODS

A. Single particle – Analytical method

We study analytically the motion of one self-propelled microscopic particle (active particle) in three-dimensions under an external force: gravity. Typically, an active particle moves inside a fluid and due to its microscopic size we cannot neglect the influence of thermal fluctuations caused by the surrounding fluid buffeting the particle. The interactions with the fluid are represented by stochastic terms as for a Brownian particle. Then, due to gravity the

* jeremy.vachier@ds.mpg.de

† marco.mazza@ds.mpg.de

suspended active particle approaches a stationary state where its position has an increased probability of being close to the confining interface. This phenomenon is called sedimentation. To describe this motion, we derive a Fokker–Planck equation [22–26].

Model — We treat the motion of one active particle in three-dimensions under gravity by considering a single active Brownian particle moving with a constant active speed v_s along a direction represented by the orientation \mathbf{e} , subject to random fluctuations. The motion of the active particle is biased by a drift velocity $-v_g \mathbf{z}$ in the direction of gravity. Our system is then described by two first-order stochastic differential equations

$$\frac{d}{dt} \mathbf{r}(t) = v_s \mathbf{e}(t) - v_g \mathbf{z} + \boldsymbol{\xi}(t), \quad (1)$$

$$\frac{d}{dt} \mathbf{e}(t) = \boldsymbol{\xi}_e(t) \times \mathbf{e}(t). \quad (2)$$

The random fluctuations are modeled in terms of white noises $\boldsymbol{\xi}$ and $\boldsymbol{\xi}_e$, defined with zero-mean Gaussian noises with variance $\langle \xi_i(t) \xi_j(t') \rangle = 2D_t \delta_{ij} \delta(t-t')$, $\langle \xi_{ei}(t) \xi_{ej}(t') \rangle = 2D_e \delta_{ij} \delta(t-t')$, where D_t and D_e are the translational and rotational diffusivities, respectively, δ_{ij} is the Kronecker delta, and $\delta(t)$ the Dirac distribution. A dimensionless measure of the relative strength of the self-propulsion to the diffusive behavior is given by the Péclet number $\mathcal{P} = v_s \sigma / D_t$, where σ is the linear size of the particle.

From Eq. (1)-(2) we can derive a Fokker–Planck equation that accounts for the evolution in time of one particle probability density function, $\mathcal{P}(\mathbf{r}, \mathbf{e}, t | \mathbf{z}a, \mathbf{e}_0, t_0)$, of finding an active particle under gravity diffusing in three-dimensions, with the initial condition $\mathcal{P}(\mathbf{r}, \mathbf{e}, t = t_0 | \mathbf{z}a, \mathbf{e}_0, t_0) = \delta(\mathbf{r} - \mathbf{z}a) \delta(\mathbf{e} - \mathbf{e}_0)$. In the following, to lighten the notation we will use $\mathcal{P}(\mathbf{r}, \mathbf{e}, t) = \mathcal{P}(\mathbf{r}, \mathbf{e}, t | \mathbf{z}a, \mathbf{e}_0, t_0)$. To derive the Fokker–Planck equation, we consider the derivative of $\mathcal{P}(\mathbf{r}, \mathbf{e}, t) = \langle \delta(\mathbf{r}(t) - \mathbf{r}) \delta(\mathbf{e}(t) - \mathbf{e}) \rangle$ with respect to time

$$\begin{aligned} \frac{\partial}{\partial t} \mathcal{P}(\mathbf{r}, \mathbf{e}, t) = & - (v_s \mathbf{e} - v_g \mathbf{z}) \cdot \nabla \mathcal{P}(\mathbf{r}, \mathbf{e}, t) - \nabla \cdot \langle \boldsymbol{\xi}(t) \delta(\mathbf{r}(t) - \mathbf{r}) \delta(\mathbf{e}(t) - \mathbf{e}) \rangle \\ & - \nabla_{\mathbf{e}} \cdot \langle [\boldsymbol{\xi}_e(t) \times \mathbf{e}] \delta(\mathbf{r}(t) - \mathbf{r}) \delta(\mathbf{e}(t) - \mathbf{e}) \rangle, \end{aligned} \quad (3)$$

where $\nabla_{\mathbf{e}} \equiv (\frac{\partial}{\partial e_x}, \frac{\partial}{\partial e_y}, \frac{\partial}{\partial e_z})^T$, where the superscript T indicates transposition. We rewrite the Itô's integral by using the Furutsu–Novikov formula [14, 16, 19, 27–31]

$$\langle \xi(t) R[\xi] \rangle = \int_{-\infty}^{+\infty} dt' \langle \xi(t) \xi(t') \rangle \left\langle \frac{\delta R[\xi]}{\delta \xi(t')} \right\rangle, \quad (4)$$

where $R[\xi]$ is an arbitrary functional of ξ . After some manipulation, we obtain the Fokker–Planck equation

$$\frac{\partial}{\partial t} \mathcal{P}(\mathbf{r}, \mathbf{e}, t) = -v_s \mathbf{e} \cdot \nabla \mathcal{P}(\mathbf{r}, \mathbf{e}, t) + v_g \frac{\partial}{\partial z} \mathcal{P}(\mathbf{r}, \mathbf{e}, t) + D_t \nabla^2 \mathcal{P}(\mathbf{r}, \mathbf{e}, t) + D_e \mathcal{L}_e \mathcal{P}(\mathbf{r}, \mathbf{e}, t), \quad (5)$$

with $\mathcal{L}_e \equiv \left[\frac{1}{\sin \theta} \frac{\partial}{\partial \theta} (\sin \theta \frac{\partial}{\partial \theta}) + \frac{1}{\sin^2 \theta} \frac{\partial^2}{\partial \phi^2} \right]$ the Laplace–Beltrami operator on the 2-sphere \mathbb{S}^2 , and we expressed $\mathbf{e} = (\sin \theta \cos \phi, \sin \theta \sin \phi, \cos \theta)^T$ in spherical coordinates.

To solve Eq. (5), we proceed in the following way: (i) we will move to Fourier space; (ii) we will use an expansion in terms of eigenfunctions of the Fokker–Planck operator; (iii) we will perform a multipole expansion; (iv) we will focus on the dependence of the probability on the the z direction, along which gravity applies; and (v) we will perform the inverse-Fourier transform. The calculations simplify considerably if we perform the Fourier transform of the distribution function

$$\widehat{\mathcal{P}}(\mathbf{k}, \mathbf{e}, t) = \int \frac{d^3 \mathbf{r}}{(2\pi)^{3/2}} e^{-i\mathbf{k} \cdot \mathbf{r}} \mathcal{P}(\mathbf{r}, \mathbf{e}, t). \quad (6)$$

The Fourier-transformed of Eq. (5) then reads

$$\frac{\partial}{\partial t} \widehat{\mathcal{P}}(\mathbf{k}, \mathbf{e}, t) = i v_s \mathbf{e} \cdot \mathbf{k} \widehat{\mathcal{P}}(\mathbf{k}, \mathbf{e}, t) - i v_g k_z \widehat{\mathcal{P}}(\mathbf{k}, \mathbf{e}, t) - D_t k^2 \widehat{\mathcal{P}}(\mathbf{k}, \mathbf{e}, t) + D_e \mathcal{L}_e \widehat{\mathcal{P}}(\mathbf{k}, \mathbf{e}, t). \quad (7)$$

The initial condition associated to Eq. (7) is simply found from

$$\widehat{\mathcal{P}}(\mathbf{k}, \mathbf{e}, t = t_0) = \frac{1}{(2\pi)^{3/2}} \int d^3 \mathbf{r} e^{-i\mathbf{k} \cdot \mathbf{r}} \mathcal{P}(\mathbf{r}, \mathbf{e}, t = t_0) = \frac{1}{(2\pi)^{3/2}} e^{-i\mathbf{k} \cdot \mathbf{z}a}. \quad (8)$$

Let us for the moment consider the case $v_s = v_g = 0$. Because the operator $\mathcal{O}_{\text{FP}} = (\frac{\partial}{\partial t} + D_t k^2 - D_e \mathcal{L}_e)$ is Hermitian, its eigenfunctions $e^{-D_t k^2 t} e^{-\lambda_n D_e t} Y_n^m(\theta, \phi)$ form an orthonormal base of the space of our solutions, where $\lambda_n = n(n+1)$, $Y_n^m(\theta, \phi) = (-1)^m \sqrt{\frac{2n+1}{4\pi} \frac{(n-m)!}{(n+m)!}} P_n^m(\cos \theta) e^{im\phi}$ are the spherical harmonics including the Condon–Shortley phase factor, and $n, m \in \mathbb{N}$, $-n \leq m \leq n$. Additionally, because $\mathcal{O}_g = iv_g k_z$ is simply a multiplicative scalar, an eigenfunction of $\mathcal{O}_{\text{FP}} + \mathcal{O}_g$ is $e^{-(iv_g k_z + D_t k^2)t} e^{-\lambda_n D_e t} Y_n^m(\theta, \phi)$. Taking into account the initial condition in Eq. (8) and the linearity of Eq. (7), we will search for solutions of the form

$$\widehat{P}(\mathbf{k}, \mathbf{e}, t) = e^{-(iv_g k_z + D_t k^2)t} e^{-ik_z a} \sum_{n=0}^{+\infty} \sum_{m=-n}^{+n} \widehat{P}_n^m(\mathbf{k}, t) e^{-D_e n(n+1)t} Y_n^m(\mathbf{e}), \quad (9)$$

where the coefficients $\widehat{P}_n^m(\mathbf{k}, t)$ have to be determined from the boundary conditions.

Inserting Eq. (9) into Eq. (7), and then multiplying by $Y_{n'}^{*m'}$ and integrating over the solid angle $d\Omega = \sin \theta d\theta d\phi$, we find

$$\frac{\partial}{\partial t} \widehat{P}_n^m(\mathbf{k}, t) = - \sum_{n'=0}^{\infty} \sum_{m'=-n'}^{+n'} \widehat{P}_{n'}^{m'}(\mathbf{k}, t) e^{-D_e(\lambda_{n'} - \lambda_n)t} \int d\Omega Y_{n'}^{m'}(\mathbf{e}) (iv_s \mathbf{e} \cdot \mathbf{k}) Y_n^{*m}(\mathbf{e}). \quad (10)$$

To proceed we define the following integrals

$$\mathcal{J}_{x_{n,n'}}^{m,m'} = \int d\Omega Y_{n'}^{m'}(\theta, \phi) \sin \theta \cos \phi Y_n^{*m}(\theta, \phi), \quad (11)$$

$$\mathcal{J}_{y_{n,n'}}^{m,m'} = \int d\Omega Y_{n'}^{m'}(\theta, \phi) \sin \theta \sin \phi Y_n^{*m}(\theta, \phi), \quad (12)$$

$$\mathcal{J}_{z_{n,n'}}^{m,m'} = \int d\Omega Y_{n'}^{m'}(\theta, \phi) \cos \theta Y_n^{*m}(\theta, \phi). \quad (13)$$

Equation (10) can be written

$$\frac{\partial}{\partial t} \widehat{P}_n^m(\mathbf{k}, t) = -iv_s \sum_{n'=0}^{\infty} \sum_{m'=-n'}^{+n'} \widehat{P}_{n'}^{m'} e^{-D_e(\lambda_{n'} - \lambda_n)t} \left[k_x \mathcal{J}_{x_{n,n'}}^{m,m'} + k_y \mathcal{J}_{y_{n,n'}}^{m,m'} + k_z \mathcal{J}_{z_{n,n'}}^{m,m'} \right]. \quad (14)$$

The calculation of the integrals $\mathcal{J}_{i_{n,n'}}^{m,m'}$ is straightforward [19]. Equation (10) becomes

$$\begin{aligned} \frac{\partial}{\partial t} \widehat{P}_n^m &= \frac{v_s}{2} e^{-2D_e(n+1)t} \left\{ (k_y - ik_x) \widehat{P}_{n+1}^{m+1} \left[\frac{(n+m+2)(n+m+1)}{(2n+3)(2n+1)} \right]^{\frac{1}{2}} - 2ik_z \widehat{P}_{n+1}^m \left[\frac{(n+m+1)(n-m+1)}{(2n+3)(2n+1)} \right]^{\frac{1}{2}} \right. \\ &+ \left. \widehat{P}_{n+1}^{m-1} \left[\frac{(n-m+2)(n-m+1)}{(2n+3)(2n+1)} \right]^{\frac{1}{2}} (k_y + ik_x) \right\} - \frac{v_s}{2} e^{2D_e n t} \left\{ (k_y - ik_x) \widehat{P}_{n-1}^{m+1} \left[\frac{(n-m)(n-m-1)}{(2n+1)(2n-1)} \right]^{\frac{1}{2}} \right. \\ &+ \left. 2ik_z \widehat{P}_{n-1}^m \left[\frac{(n+m)(n-m)}{(2n+1)(2n-1)} \right]^{\frac{1}{2}} + (k_y + ik_x) \widehat{P}_{n-1}^{m-1} \left[\frac{(n+m)(n+m-1)}{(2n+1)(2n-1)} \right]^{\frac{1}{2}} \right\} \end{aligned} \quad (15)$$

We are interested in the dynamics along the direction of gravity, the z direction; hence we specialize the previous equation to this case. The general equation for the coefficients \widehat{P}_n^m reads

$$\frac{\partial}{\partial t} \widehat{P}_n^m = -v_s ik_z \left\{ e^{-2D_e(n+1)t} \widehat{P}_{n+1}^m \left[\frac{(n+m+1)(n-m+1)}{(2n+3)(2n+1)} \right]^{\frac{1}{2}} + e^{2D_e n t} \widehat{P}_{n-1}^m \left[\frac{(n+m)(n-m)}{(2n+1)(2n-1)} \right]^{\frac{1}{2}} \right\}. \quad (16)$$

Because of the rotational dynamics in our problem, it is convenient to explicitly highlight the underlying symmetries by expanding the full probability $\mathcal{P}(\mathbf{r}, \mathbf{e}, t)$ in terms of spherical tensors, the irreducible representations of the rotation operator. Each spherical tensor transforms like the eigenfunctions of the angular momentum of corresponding rank $n = 0, 1, 2, \dots$, where the first three tensors represent the density ρ (monopole, $n = 0$), the polarization \mathbf{J} (dipole, $n = 1$), and the nematic tensor \mathbf{Q} (quadrupole, $n = 2$), respectively. The probability can then be expanded as

$$\mathcal{P}(\mathbf{r}, \mathbf{e}, t) = \rho(\mathbf{r}, t) + \mathbf{J}(\mathbf{r}, t) \cdot \mathbf{e} + \mathbf{e} \cdot \mathbf{Q}(\mathbf{r}, t) \cdot \mathbf{e} + \dots \quad (17)$$

In the large time limit, the monopole term $\rho(\mathbf{r}, t)$ will dominate the sedimentation process. Its Fourier transform can be found by truncating the sum in Eq. (9) at the $n = 0$ term, that is

$$\hat{\rho}(k_z, t) = \frac{1}{\sqrt{4\pi}} e^{-(iv_g k_z t + D_t k_z^2)t} e^{-ik_z a} \hat{P}_0^0. \quad (18)$$

To find \hat{P}_0^0 , we use the (16) and after some computations (see Appendix), we obtain

$$\frac{\partial^2}{\partial t^2} \hat{P}_0^0 + 2D_e \frac{\partial}{\partial t} \hat{P}_0^0 + \frac{v_s^2}{3} k_z^2 \hat{P}_0^0 = 0, \quad (19)$$

which is the telegrapher's equation [32].

A solution of Eq. (19) reads $\hat{P}_0^0(k_z, t) = e^{-D_e t} [\hat{F}(k_z) e^{-iw(k_z)t} + \hat{G}(k_z) e^{iw(k_z)t}]$, where $w(k_z) = (k_z^2 \frac{v_s^2}{3} - D_e^2)^{1/2}$, with $\hat{G}(k_z)$ and $\hat{F}(k_z)$ arbitrary functions of the wavevector in the z direction k_z . The expression for the monopole is found from the inverse Fourier transform, and reads

$$\rho(z, t) = \int_{-\infty}^{+\infty} \frac{dk_z}{\sqrt{2\pi}} \hat{\rho}(k_z, t) e^{ik_z z} = \frac{e^{-D_e t}}{\pi\sqrt{8}} \int_{-\infty}^{+\infty} dk_z e^{-iv_g k_z t - D_t k_z^2 t} e^{-ik_z a} e^{ik_z z} [\hat{F}(k_z) e^{-iw(k_z)t} + \hat{G}(k_z) e^{iw(k_z)t}].$$

The functions $\hat{F}(k_z)$ and $\hat{G}(k_z)$ are arbitrary and we choose $F(z) = G(z) = 1$ for the sake of simplicity. The term $w(k_z) = (k_z^2 \frac{v_s^2}{3} - D_e^2)^{1/2}$ in the exponential makes it difficult to perform the inverse Fourier transform. However, we are interested in the long-wavelength limit of the sedimentation profile, so it is natural to consider a Taylor expansion of $w(k_z)$ around $k_z = 0$

$$\rho(z, t) = \frac{e^{-D_e t}}{\pi\sqrt{8}} \int_{-\infty}^{+\infty} dk_z e^{-D_t k_z^2 t - iv_g k_z t} e^{ik_z z} e^{-ik_z a} \left[e^{-D_e t + \frac{v_s^2 k_z^2}{6D_e}} + e^{D_e t - \frac{v_s^2 k_z^2}{6D_e}} \right].$$

Elementary integration yields

$$\rho(z, t) = \frac{1}{\sqrt{8\pi}} \left\{ e^{-2D_e t} \frac{1}{\sqrt{D_{\text{eff}}^- t}} e^{-(z-a-v_g t)^2 / (4D_{\text{eff}}^- t)} + \frac{1}{\sqrt{D_{\text{eff}}^+ t}} e^{-(z-a-v_g t)^2 / (4D_{\text{eff}}^+ t)} \right\}, \quad (20)$$

where we have defined effective diffusivities $D_{\text{eff}}^{\pm} \equiv D_t \pm \frac{v_s^2}{6D_e}$. That active motion enhances diffusion has been repeatedly observed in experimental results [11].

In order to describe sedimentation, we need to impose a reflective boundary condition due to the confining wall located at $z = 0$. We use the method of images, which consists of replacing the wall at $z = 0$ with a mirror source placed at $z = -a$ (in addition to the real source at $z = a$) such that the solution for the probability density function $\rho(z, t|a)$ from the original and mirror sources compensate at the wall at any time [33]. Generally, due to the linearity of the Fokker-Planck Eq. (5) the solution in the presence of a reflective boundary ρ_r can be written as a superposition of solutions in an unbounded domain, *i.e.*, $\rho_r(z, t|a) = \rho(z, t|a) + e^{\beta} \rho(z, t|-a)$, where e^{β} determine the strength of the mirror image source. In order to find the mirror image strength we apply the condition of null flux, *i.e.*, $\frac{\partial}{\partial z} \rho_r(z, t|a)|_{z=0} = 0$, and obtain

$$\rho_r(z, t|a) = \rho(z, t|a) + \left\{ \frac{(a + tv_g) A e^{-\frac{3}{2}A(a+tv_g)^2} - B e^{-\frac{3}{2}B(a+tv_g)^2}}{(a - tv_g) A e^{-\frac{3}{2}A(a-tv_g)^2} - B e^{-\frac{3}{2}B(a-tv_g)^2}} \right\} \rho(z, t|-a), \quad (21)$$

where $A \equiv \left[\frac{D_e}{t(6D_t D_e + v_s^2)} \right]^{\frac{3}{2}}$, $B \equiv \left[\frac{D_e}{t(6D_t D_e - v_s^2)} \right]^{\frac{3}{2}}$. Our choice of initial and boundary conditions has the effect that when v_g takes on negative values it is aligned with gravity.

Our result is similar to the simple case of a one-dimensional Wiener process with a drift term and in the presence of a wall at $z = 0$ [34]. This highlights the robustness of our model. The next step is to describe the sedimentation process for a many-particle system. An analytical approach is a formidable task; thus we turn to numerical simulations.

In the following, we express all physical quantities by taking the active particle's diameter σ , mass m and its translational diffusion coefficient D_t as the units of length, mass and diffusivity. Thus, we can measure all the others quantities in terms of those three units, *e.g.*, time in units of $\tilde{t} = \sigma^2/D_t$, and rotational diffusivity in terms of $\tilde{D}_e = D_t/\sigma^2$.

B. Collective motion – Simulations

In order to study the collective motion of many active particles in three dimensions (3D), we perform molecular dynamics simulations. Due to the size of the active particles, *e.g.* the microalga *Chlamydomonas reinhardtii* has a typical length $\sigma = 10 \mu\text{m}$ and self-propulsion speed $v_s = 60 \mu\text{m/s}$, the Reynolds number $\mathcal{R} \ll 1$. As in Sec. II A, we describe the system by using two first-order stochastic differential equations, for N active particles

$$\frac{d}{dt} \mathbf{r}_i = v_s \mathbf{e}_i - \nabla \phi_{WCA} - v_g \hat{\mathbf{z}} + \boldsymbol{\xi}_i, \quad (22)$$

$$\frac{d}{dt} \mathbf{e}_i = \boldsymbol{\xi}_{e_i} \times \mathbf{e}_i - \gamma \frac{\partial U}{\partial \mathbf{e}_i}, \quad (23)$$

where $i = 1, \dots, N$, $\|\mathbf{e}_i\| = 1$ (implemented by means of a Lagrangian multiplier), v_g is the limiting velocity of a particle in the fluid under gravitational acceleration. In Eq. (22), $\phi_{WCA} = 4\epsilon[(\sigma/r_{ij})^{12} - (\sigma/r_{ij})^6] + \epsilon$ is the Weeks–Chandler–Anderson potential [35], representing a hard-core repulsion between active particles, where σ is the linear size of the active particles. In Eq. (23), $U = \sum_{i \neq j} \cos^2(\theta_{ij})$ is the Lebwohl-Lasher potential, which we use to model to first approximation the up-down symmetric interaction due to hydrodynamics that tends to align neighboring particles.

We integrate Eqs. (22)-(23) with a discretization scheme based on the Euler–Maruyama algorithm in which we take into account the issue of multiplicative noise. We solve Eq. (22)-(23) in a domain of volume $V = L^3$, with $L = 50\sigma$, with a reflective wall at the bottom at $z = 0$, and gravity pointing in negative z -direction.

III. RESULTS

A. Analytical method

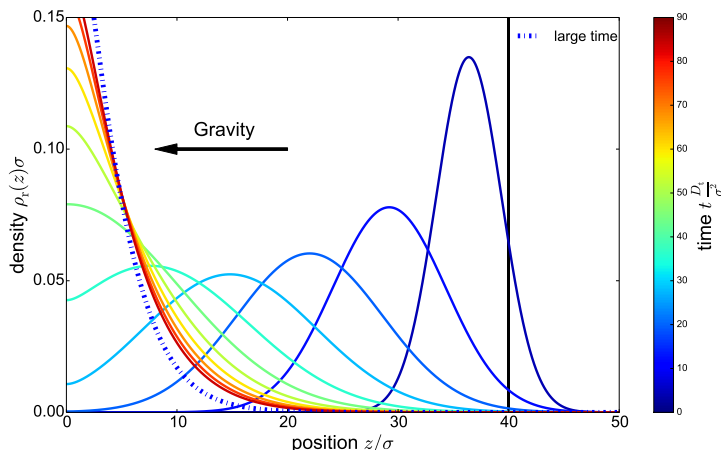


Figure 1. Dependence of the density $\rho_r(z)$ on the position z , computed from Eq. (21), at different times for a system with one active particle under gravity in a cubic box of linear size $L = 50\sigma$ with wall on bottom ($z = 0$) and with gravity pointing in negative z -direction. At $t = 0$, the initial position of the active particle is at $z/\sigma = 40$, and the corresponding probability density is a Dirac delta distribution. With time we observe a spreading of the density profile and a shift in the direction of gravity. For large time, we obtain a sedimentation profile characterised by an exponential decay with distance. Different curves correspond to different moments during the time evolution. The model parameters are $v_s/v_g = 1.1$, and $D_e D_t / \sigma^2 = 1.8$.

Figure 1 shows the evolution of the density profile $\rho_r(z, t)$ found from our solution to the sedimentation process in Eq. (21). The initial position of the active particle is chosen at $z/\sigma = 40$. The corresponding initial density $\rho_r(z, t = 0)$ is a Dirac delta distribution. As time progresses, we observe the shifting and flattening of the density profile. Finally, the active particle sediments on the bottom wall. At large times the sedimentation profile is characterized by an exponential dependence on position.

Figure 2 shows the dependence of the normalized density profile at large times upon variation of the effective diffusion coefficient $D_{\text{eff}} = D_{\text{eff}}^+$. Detailed experiments on the sedimentation of active particles were performed by

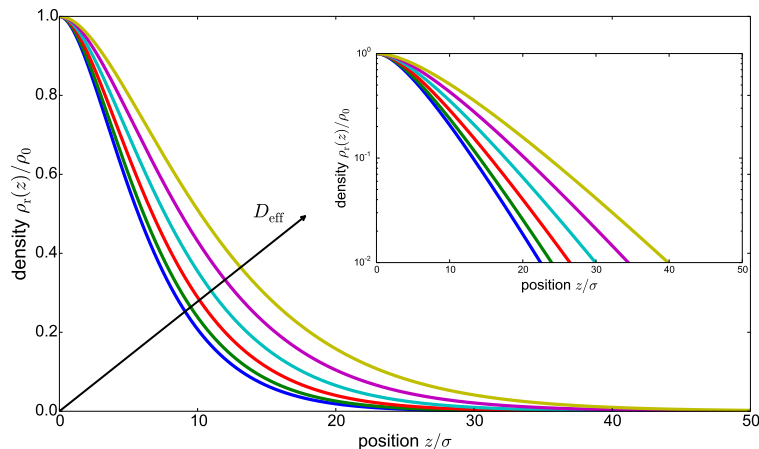


Figure 2. Dependence of the normalized density $\rho_r(z)/\rho_0$ on the position z , computed from Eq. 21, for different values of the effective diffusion coefficient $D_{\text{eff}} = D_t + \frac{v_s^2}{6D_e}$; each curve corresponds to the long time behavior of the sedimentation process, and $\rho_0 = \rho_r(z=0)$. We observe a good match with the experimental results in [11]. The model parameters are $D_e\sigma^2/D_t = 1.8$, $v_s/v_g \in [1.25, 10.0]$.

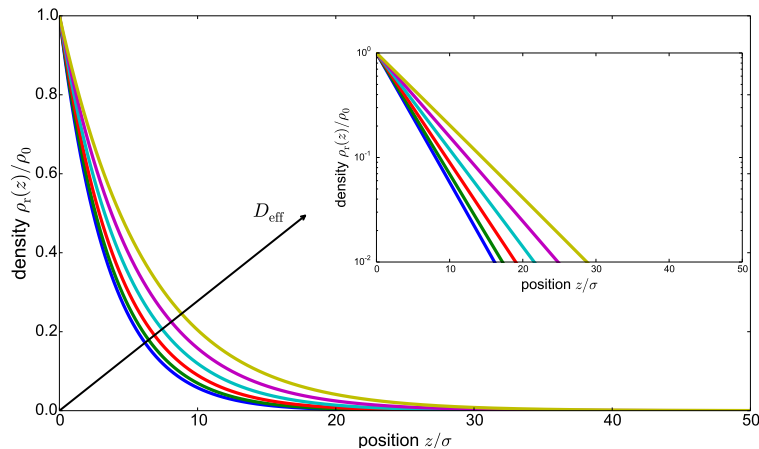


Figure 3. Dependence of the normalized density $\rho_r(z)/\rho_0$ on the position z , computed from Eq. 21 but where the strength of the mirror image was set equal to one. Different curves correspond to the long time behavior of the sedimentation process for different values of the effective diffusion coefficient $D_{\text{eff}} = D_t + \frac{v_s^2}{6D_e}$. We observe a good match with the experimental results in [11]. The model parameters are $D_e\sigma^2/D_t = 1.8$, and $v_s/v_g \in [1.2, 6.6]$.

Palacci *et al.* [11], where 1 μm -sized active Janus colloids self-propel due to chemical reactions with a solution of H_2O_2 . As in the experiments [11], we fix both the translational diffusion coefficient D_t and the rotational diffusion coefficient D_e , and we vary the self-propulsion speed v_s . We match our parameters with the experimental values given in [11], where the Péclet number $0.5 \lesssim \mathcal{P} \lesssim 5$, and we find a near-quantitative agreement with the experiments.

As predicted in theoretical works [18, 20], $\rho_r(z)$ decays exponentially away from the confining surface. We note, however, a small deviation from strict exponential behavior very close to the surface. We can recover an exact exponential decay by changing the strength of the mirror image, as shown in Fig. 3. Experimental data in close proximity of the confining surface are missing, so it does not seem possible to discriminate between the two scenarios shown in Fig. 2 and 3. In any case, the precise nature of the density profile in proximity to the confining surface will be affected by a number of effects—such as hydrodynamic interactions with the walls, near-field hydrodynamics, steric effects, electrostatics—that we do not account for here.

The sedimentation length δ_{eff} is the characteristic length scale of the decay of $\rho_r(z, t)$ with z . It was found to depend strongly on the activity of the self-propelling particle [11, 18]. Figure 4 shows a test of the relation between δ_{eff} and D_{eff} . In general, we find a linear relationship governing the growth of δ_{eff} with D_{eff}/v_g , $\delta_{\text{eff}} = c_0 + D_{\text{eff}}/v_g$.

The constant $c_0 \equiv c_0(v_g)$, and can be chosen to be zero, which is the value consistent with the experiments in [11]. We can conclude that we find good agreement with the experiments.

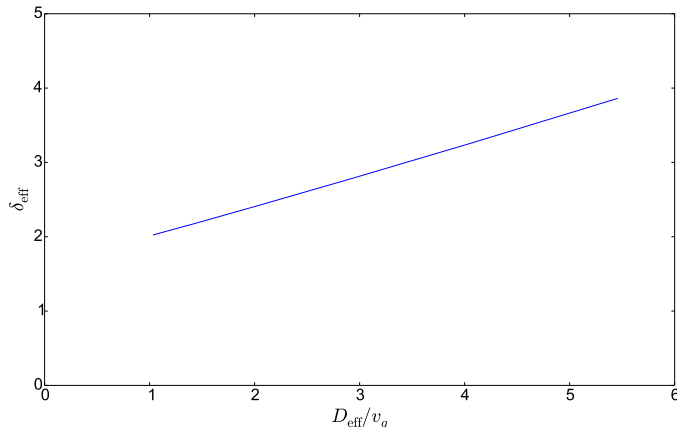


Figure 4. Dependence of the sedimentation length on the effective diffusivity. The analytical calculations predict a linear dependence, that agrees with the experimental results in [11]. The model parameters are $D_e\sigma^2/D_t = 1.8$, $v_s/v_g \in [0.4, 3.6]$.

B. Simulations

To explore the effect of weak hydrodynamic interactions among active particles on their sedimentation, we also address a system of $N = 10^3$ active particles under gravity, with the same geometry as above. Our results shown below are averaged over 10^4 independent simulations. Figure 5 shows the dependence of the density profile $\rho_r(z)$ on the position z at different times. At $t = 0$, the active particles are randomly placed on a plane placed at $z/\sigma = 40$. After some time, all the active particles sediment on the bottom wall. We observe a qualitative agreement of our simulation with the theory in Sec. II A. We conclude that, as long as hydrodynamic interactions are weak, or the system diluted enough, the theory derived for a single active particle is applicable also to a many-particle system.

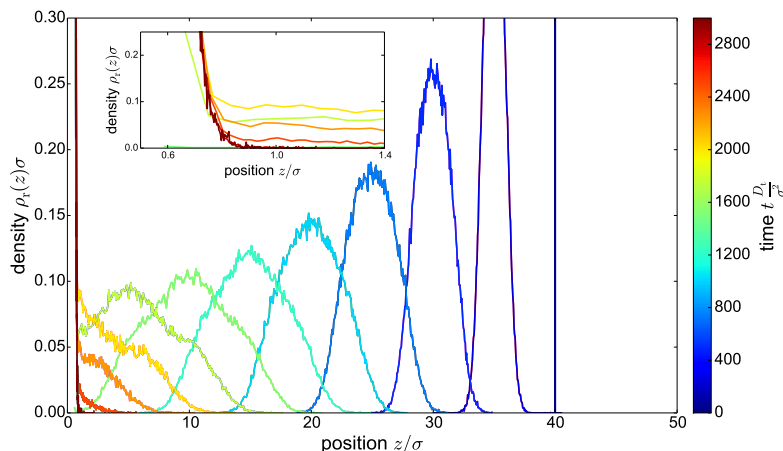


Figure 5. Dependence of the density $\rho_r(z)$ on the position z at different times from simulations of $N = 1000$ active particle in a cubic box of linear size $L = 50\sigma$ with a wall on bottom ($z = 0$) and with gravity pointing in negative z -direction. Results are averaged over 10^4 independent simulations. At $t = 0$, the active particles are randomly placed on a plane placed at $z/\sigma = 40$. Different curves correspond to different moments during the time evolution. The model parameters are $v_s/v_g = 0.2$.

To measure the importance of the active motion with respect to the diffusion, we vary the Péclet number \mathcal{P} by changing the self-propulsion v_s . Figure 6 shows the results of our simulations for the density profile at large t , and at different values of self-propulsion v_s . When the activity is lower than the sedimentation velocity, $v_s/v_g = 0.2$, we

observe a clear sedimentation profile. If $v_s/v_g = 1.0$, we observe a weaker sedimentation profile and a peak appears on the upper part of the simulated domain. This peak is due to balance of the weak hydrodynamic interactions introduced in our simulations with the self-propulsion and the effect of gravity. In a similar setting, an emerging polar order in sedimenting active particles was predicted in [8]. Finally, as soon as $v_s > v_g$, we observe an accumulation of particles both on the bottom and top end.

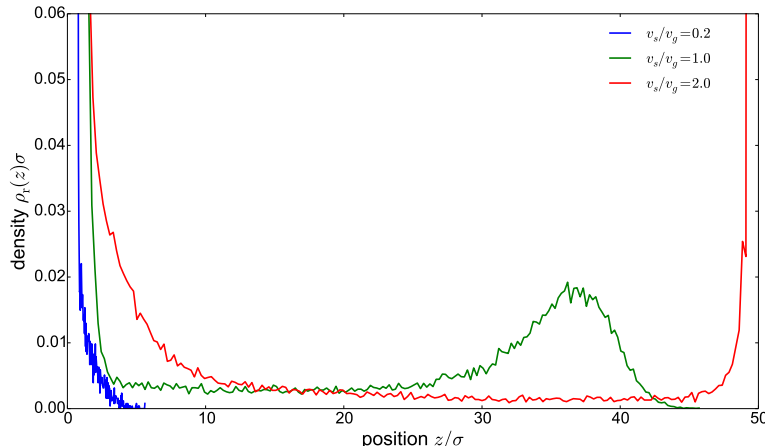


Figure 6. Dependence of the density $\rho_r(z)$ on the position z for a system with $N = 1000$ active particle, for large t . Different curves correspond to different values of v_s/v_g .

IV. CONCLUSION

We study the sedimentation process of active particles in three-dimensions. Firstly, we develop an analytical method describing the sedimentation profile of one active particle. We solve analytically the Fokker–Planck equation for an active particle in the presence of gravity and a confining wall at the bottom. We recover the following experimental results found in [11, 12]: (i) the exponentially decaying density profile at large times (ii) the increasing sedimentation length upon increase of the effective diffusivity, as shown in Fig. 4. Importantly, our method retains the full temporal dynamics of the sedimentation process, and therefore in addition to the limit of large times (steady state) we also have access to the intermediate states. Our method also allows us to keep the coupling between the orientational and the positional degrees of freedom. In order to characterize more realistic conditions for the sedimentation process, we also consider many particles with weak hydrodynamic interactions and we carry out molecular dynamics simulations. We are able to measure the importance of the active motion at large times by varying the Péclet number \mathcal{P} . We recover the density profile, shown in Fig. 6, found experimentally in [12] and in numerical simulations [18] of active bottom-heavy particles. However, our model allows us to characterize more in details the richness of the sedimentation process of active particles as function of the activity. Furthermore, the sedimentation profile predicted by our analytical method for one active particle (see Fig. 2) matches our simulations for many particles (see Fig. 5).

Future work will address how hydrodynamic interactions among active particles affect the collective dynamics by explicitly including a fluid.

ACKNOWLEDGMENTS

We gratefully acknowledge Soumyajyoti Biswas, Stephan Herminghaus, and Rebekka Breier for helpful conversations. We thank the Max Planck Society and the Max Planck Center for Complex Fluid Dynamics for funding.

Appendix A: Telegrapher's equation

Here we provide details of the computation of the telegrapher's equation (19). We start by considering the equations for the two coefficients \hat{P}_0^0 and \hat{P}_1^0

$$\frac{\partial}{\partial t} \hat{P}_0^0 = -\frac{v_s}{\sqrt{3}} e^{-2D_e t} i k_z \hat{P}_1^0, \quad (\text{A1})$$

$$\frac{\partial}{\partial t} \hat{P}_1^0 = -v_s e^{-4D_e t} \sqrt{\frac{4}{15}} i k_z \hat{P}_2^0 - \frac{v_s}{\sqrt{3}} e^{2D_e t} i k_z \hat{P}_0^0, \quad (\text{A2})$$

combining these two Eqs. yields

$$\frac{\partial^2}{\partial t^2} \hat{P}_0^0 = 2D_e \frac{v_s}{\sqrt{3}} e^{-2D_e t} i k_z \hat{P}_1^0 - \frac{v_s}{\sqrt{3}} e^{-2D_e t} i k_z \frac{\partial}{\partial t} \hat{P}_1^0, \quad (\text{A3})$$

and after replacing the last term on the right hand side with Eq. (A2) we find

$$\frac{\partial^2}{\partial t^2} \hat{P}_0^0 + 2D_e \frac{\partial}{\partial t} \hat{P}_0^0 + \frac{v_s^2}{3} k_z^2 \hat{P}_0^0 = -v_s^2 \sqrt{\frac{4}{45}} k_z^2 \hat{P}_2^0 e^{-6D_e t}.$$

Finally, taking the limit $t \rightarrow \infty$ yields

$$\frac{\partial^2}{\partial t^2} \hat{P}_0^0 + 2D_e \frac{\partial}{\partial t} \hat{P}_0^0 + \frac{v_s^2}{3} k_z^2 \hat{P}_0^0 = 0,$$

which is the telegrapher's Eq. (19).

- [1] J. Elgeti, R. G. Winkler, and G. Gompper, Rep. Prog. Phys. **78**, 056601 (2015).
- [2] A. Ghosh and P. Fischer, Nano Lett. **9**, 2243 (2009).
- [3] S. Kim, F. Qiu, S. Kim, A. Ghanbari, C. Moon, L. Zhang, B. J. Nelson, and H. Choi, Adv. Mat. **25**, 5863 (2013).
- [4] C. C. Maass, C. Krüger, S. Herminghaus, and C. Bahr, Annu. Rev. Condens. Matter Phys. **7**, 171 (2016).
- [5] C. Krüger, G. Klös, C. Bahr, and C. C. Maass, Phys. Rev. Lett. **117**, 048003 (2016).
- [6] C. Jin, C. Krüger, and C. C. Maass, Proc. Natl. Acad. Sci. USA **114**, 5089 (2017).
- [7] R. Golestanian, Phys. Rev. Lett. **102**, 188305 (2009).
- [8] M. Enculescu and H. Stark, Phys. Rev. Lett. **107**, 058301 (2011).
- [9] B. Ten Hagen, F. Kümmel, R. Wittkowski, D. Takagi, H. Löwen, and C. Bechinger, Nature Commun. **5**, 4829 (2014).
- [10] A. I. Campbell, R. Wittkowski, B. ten Hagen, H. Löwen, and S. J. Ebbens, J. Chem. Phys. **147**, 084905 (2017).
- [11] J. Palacci, C. Cottin-Bizonne, C. Ybert, and L. Bocquet, Phys. Rev. Lett. **105**, 088304 (2010).
- [12] F. Ginot, I. Theurkauff, D. Levis, C. Ybert, L. Bocquet, L. Berthier, and C. Cottin-Bizonne, Phys. Rev. X **5**, 011004 (2015).
- [13] P. Romanczuk, M. Bär, W. Ebeling, B. Lindner, and L. Schimansky-Geier, Eur. Phys. J. Special Topics **202**, 1 (2012).
- [14] F. J. Sevilla and M. Sandoval, Phys. Rev. E **91**, 052150 (2015).
- [15] A. Pototsky and H. Stark, EPL (Europhysics Letters) **98**, 50004 (2012).
- [16] F. J. Sevilla and L. A. Gómez Nava, Phys. Rev. E **90**, 022130 (2014).
- [17] C. G. Wagner, M. F. Hagan, and A. Baskaran, J. Stat. Mech. **2017**, 043203 (2017).
- [18] K. Wolff, A. M. Hahn, and H. Stark, Eur. Phys. J. E **36**, 43 (2013).
- [19] F. J. Sevilla, Phys. Rev. E **94**, 062120 (2016).
- [20] J. Tailleur and M. E. Cates, EPL (Europhysics Letters) **86**, 60002 (2009).
- [21] C. Kurzthaler, S. Leitmann, and T. Franosch, Sci. Rep. **6**, 36702 (2016).
- [22] N. V. Kampen, *Stochastic Processes in Physics and Chemistry* (North Holland; 3 edition, 23 April 2007).
- [23] C. Gardiner, *Handbook of Stochastic Methods* (Springer-Verlag Berlin Heidelberg, 1983).
- [24] H. Risken, *The Fokker-Planck Equation* (Springer-Verlag Berlin Heidelberg, 1984).
- [25] T. D. Frank, *Nonlinear Fokker-Planck Equations* (Springer-Verlag Berlin Heidelberg, 2005).
- [26] G. A. Pavliotis, *Stochastic Processes and Applications Diffusion Processes, the Fokker-Planck and Langevin Equations* (Springer-Verlag New York, 2014).
- [27] V. I. Klyatskin, *Stochastic Equations: Theory and Applications in Acoustics, Hydrodynamics, Magnetohydrodynamics, and Radiophysics, Volume 1* (Springer International Publishing Switzerland, 2015).
- [28] V. V. Konotop and L. Vazquez, *Nonlinear Random Waves* (World Scientific, Singapore, 1994).
- [29] T. D. Frank, Phys. Rev. E **71**, 031106 (2005).

- [30] E. A. Novikov, J. Exptl. Theoret. (URSS) Phys. **20** (1964).
- [31] J. Zinn-Justin, *Quantum field theory and critical phenomena* (Clarendon Press, 2002).
- [32] V. Ilyin, I. Procaccia, and A. Zagorodny, Condensed Matter Phys. **16**, 13004 (2013).
- [33] S. Redner, *A guide to first-passage processes* (Cambridge University Press, 2001).
- [34] D. R. S. Geoffrey R. Grimmett, *One Thousand Exercises in Probability* (Oxford university press - first edition, 2001).
- [35] J. D. Weeks, D. Chandler, and H. C. Andersen, J. Chem. Phys. **54**, 5237 (1971).